PHOTOSYNTHETICA
International Journal for Photosynthesis Research

DOI 10.32615/ps.2022.016 PHOTOSYNTHETICA 60 (1): 147-156, 2022

Special issue in honor of Prof. George C. Papageorgiou

Dependence of the rate-limiting steps in the dark-to-light transition of photosystem II on the lipidic environment of the reaction center

M. MAGYAR[*], P. AKHTAR[*], G. SIPKA[*], W. HAN[**], X. LI[**], G. HAN[**], J.-R. SHEN[**,***], P.H. LAMBREV[*,+], and G. GARAB[*,#,+]

Institute of Plant Biology, Biological Research Centre, Szeged, Hungary[*]
Photosynthesis Research Center, Key Laboratory of Photobiology, Institute of Botany, Chinese Academy of Sciences, Beijing, China[**]
Research Institute for Interdisciplinary Science and Graduate School of Natural Science and Technology, Okayama University, Okayama, Japan[***]
Faculty of Science, University of Ostrava, Ostrava, Czech Republic[#]

Abstract

In our earlier works, we have identified rate-limiting steps in the dark-to-light transition of PSII. By measuring chlorophyll *a* fluorescence transients elicited by single-turnover saturating flashes (STSFs) we have shown that in diuron-treated samples an STSF generates only F_1 (< F_m) fluorescence level, and to produce the maximum (F_m) level, additional excitations are required, which, however, can only be effective if sufficiently long $\Delta\tau$ waiting times are allowed between the excitations. Biological variations in the half-rise time ($\Delta\tau_{1/2}$) of the fluorescence increment suggest that it may be sensitive to the physicochemical environment of PSII. Here, we investigated the influence of the lipidic environment on $\Delta\tau_{1/2}$ of PSII core complexes of *Thermosynechococcus vulcanus*. We found that while non-native lipids had no noticeable effects, thylakoid membrane lipids considerably shortened the $\Delta\tau_{1/2}$, from ~ 1 ms to ~ 0.2 ms. The importance of the presence of native lipids was confirmed by obtaining similarly short $\Delta\tau_{1/2}$ values in the whole *T. vulcanus* cells and isolated pea thylakoid membranes. Minor, lipid-dependent reorganizations were also observed by steady-state and time-resolved spectroscopic measurements. These data show that the processes beyond the dark-to-light transition of PSII depend significantly on the lipid matrix of the reaction center.

Keywords: closed state of PSII; conformational changes; dielectric relaxation; light-adapted state of PSII, light-induced changes; proteoliposomes.

Highlights

- Structural–functional flexibility of PSII depends largely on thylakoid lipids
- The lipid matrix of PSII affects the rate-limiting steps in the dark-to-light transition
- PSII proteoliposomes assembled with native lipids are similar to the thylakoid membrane

Received 16 December 2021
Accepted 7 March 2022
Published online 14 March 2022

[+]Corresponding authors
e-mail: lambrev.petar@brc.hu
garab.gyozo@brc.hu

Acknowledgments: The authors acknowledge the support from the Hungarian Ministry of Innovation and Technology, National Research, Development, and Innovation Fund (OTKA grants K-128679 to G.G.; PD-121225 to M.M.; PD-138498 to G.S.; FK-139067 to P.A., who also used support from the grant of Eötvös Loránd Research Network SA-76/2021). P.H.L. used support from the grant 2018-1.2.1-NKP-2018-00009. G.G. also acknowledges the support from the Czech Science Foundation (GA ČR 19-13637S), and the Eötvös Loránd Research Network (ELKH KÖ-36/2021). Studies in the Chinese group are supported by a National Key R&D Program of China (2017YFA0503700), CAS Project for Young Scientists in Basic Research (YSBR-004), a Strategic Priority Research Program of the Chinese Academy of Sciences (XDB17000000), and a National Natural Science Foundation of China (31470339). The authors would like to thank András Kincses for technical support with dynamic light scattering measurements.
Conflict of interest: The authors declare that they have no conflict of interest.

Introduction

Photosystem II is a multisubunit membrane protein complex, the only enzymatic complex able to perform the oxidation of water. It catalyses electron transport from the water-splitting complex (or OEC, the oxygen-evolving complex) to plastoquinone at its Q_B site (Cardona *et al.* 2012). The RC contains the D1/D2 proteins, which bind all the cofactors required for the primary charge separation. Upon illumination of a dark-adapted open-state PSII ($PSII_O$), electron transfer from the excited primary donor P_{680}^* to Pheo forms the $P_{680}^+/Pheo^-$ radical pair within tens of picoseconds (note that P_{680}^* refers to a singlet excited state shared among several chlorins, whereas the radical cation is primarily chlorophyll P_{D1}), subsequent electron-transfer steps – from $Pheo^-$ to Q_A, the first quinone electron acceptor, and from a tyrosine residue (Y_Z) on the D1 protein to P_{680}^+ – stabilize the charge-separated state. These reactions on the acceptor and donor sides occur on the timescale of 200–300 ps and about 30 ns, respectively (Brettel *et al.* 1984, Nuijs *et al.* 1986, Rutherford 1989, Hansson and Wydrzynski 1990). Y_Z then oxidizes the Mn_4CaO_5 cluster of the OEC. This charge-separated state, with all Q_A reduced, is a closed state of PSII ($PSII_C$), which is followed by slower electron-transfer reactions between the primary and the secondary quinone acceptors, Q_A and Q_B.

Chlorophyll *a* (Chl *a*) fluorescence is one of the most widely used techniques to monitor the functioning of PSII and the photosynthetic activity of oxygenic photosynthetic organisms (Papageorgiou and Govindjee 2004, 2011). It is a noninvasive technique, which can be used both in the laboratory and field or even space conditions, from isolated PSII preparations to whole plants and large ecosystems. With different techniques, Chl *a* fluorescence induction and relaxation kinetics provide information, among others, on the kinetics of electron transfer reactions in PSII, the redox state of the plastoquinone pool, PSII activity, state transitions, the effects of electron transport inhibitors and electron donors and acceptors, photoinhibition and repair mechanisms, responses to biotic and abiotic stresses, and about the utilization or dissipation of the absorbed excitation energy (Schreiber *et al.* 1995, Strasser *et al.* 1995, Horton and Ruban 2005, Tóth *et al.* 2007, Prášil *et al.* 2018). However, the interpretation of the complex fluorescence induction kinetics is not free from controversies (Vredenberg and Prasil 2013, Kalaji *et al.* 2014, Schansker *et al.* 2014, Laisk and Oja 2020, Oja and Laisk 2020).

In our earlier work, by investigating Chl *a* fluorescence transients, elicited by trains of single-turnover saturating flashes, we discovered rate-limiting steps in the dark-to-light transition of PSII (Magyar *et al.* 2018). We showed that, following Joliot and Joliot (1979), the fluorescence level of closed RCs, generated by the first STSF, displayed an $F_1 < F_m$ fluorescence level, and the fluorescence maximum (F_m) in the presence of *N*′-(3,4-dichlorophenyl)-*N*,*N*-dimethylurea (DCMU) could only be reached gradually by several (or, as shown by us, at cryogenic temperatures, by a large number of) STSFs or by long multiple-turnover saturating flashes (MTSFs). The results of Joliot and Joliot (1979) served as the starting point of the experiments of Magyar *et al.* (2018) which led to the recognition that no (F_1-to-F_2-to-F_3-…-F_m) fluorescence rise could be obtained without sizeable waiting times ($\Delta\tau$) between consecutive STSFs. Magyar *et al.* (2018) determined the $\Delta\tau_{1/2}$ values in different PSII(-containing) preparations and under a variety of experimental conditions.

There are numerous observations in the literature from which it can be inferred that waiting times are required to complete the F_v variable fluorescence ($F_v = F_m - F_0$). However, most data were interpreted within the frameworks of the widely accepted model, the Q_A model, according to which 'to reach [F_m], it is necessary, and sufficient, to have Q_A completely reduced in all the active PSII centers'. The main observations are listed and discussed as follows: (*1*) As already mentioned, Joliot and Joliot (1979) showed that F_m cannot be reached upon reducing Q_A (Q_1) with an STSF and several additional flashes were required – after the stabilization of the charge-separated state – to complement F_v in the presence of DCMU. The consecutive reactions, which were nonelectrogenic, were attributed to the operation of a second hypothetic quencher molecule (Q_2). Later experiments made efforts to identify Q_2; however, its existence has recently been ruled out (Magyar *et al.* 2018, Sipka *et al.* 2021). (*2*) Valkunas *et al.* (1991) and France *et al.* (1992) showed that the kinetics of the fast fluorescence rise depended on the length of the excitation flashes rather than on their intensity: sub-nanosecond flashes induced exponential rise while microsecond to millisecond flashes produced sigmoidal kinetic rise. These data were interpreted – using the Q_A model – to reflect variations in the energetic coupling between PSII units; the sigmoidal rise was ascribed to the connectivity of PSII units (Lavergne and Trissl 1995, Stirbet 2013). However, the sigmoidal rise – as pointed out by Vredenberg (2008) – might also originate from two overlapping exponential kinetic components. Magyar *et al.* (2018) and Sipka *et al.*

Abbreviations: Chl *a* – chlorophyll *a*; CD – circular dichroism; CMC – critical micelle concentration; CP43 and CP47 – core antenna proteins of PSII; DAES – decay-associated emission spectra; DCMU – *N*′-(3,4-dichlorophenyl)-*N*,*N*-dimethylurea; DGDG – digalactosyldiacylglycerol; F_0 – minimum fluorescence yield; F_1, F_2 – fluorescence yield after the first, second STSF; F_m – maximal fluorescence yield; F_v – variable chlorophyll *a* fluorescence; MGDG – monogalactosyldiacylglycerol; MTSF – multiple-turnover saturating flash; OEC – oxygen-evolving complex; P_{680} – primary donor of PSII; PC – phosphatidylcholine; PE – phosphatidylethanolamine; PG – phosphatidylglycerol; Pheo – first pheophytin electron acceptor of PSII; $PSII_C$ – closed state of PSII; PSII CC – PSII core complex; $PSII_L$ – light-adapted charge-separated state of PSII; $PSII_O$ – open-state PSII; RC – reaction center; RT – room temperature; SQDG – sulfoquinovosyldiacylglycerol; STSF – single-turnover saturating flash; TM – thylakoid membrane; Y_Z – tyrosine residue of PSII; β-DDM – n-dodecyl-β-maltoside; $\Delta\tau$ – waiting time between excitations; $\Delta\tau_{1/2}$ – half-rise time of the waiting time between STSFs to complete the F_1-to-F_2 fluorescence rise.

(2019, 2021) have shown that several, at cryogenic temperatures a very large number of consecutive light-induced events, are involved in F_v. Further, it has been demonstrated, *via* recording fast Chl *a* fluorescence induction kinetics, that DCMU-treated monomeric PSII CCs display sigmoidal rise – showing that this complex fluorescence rise kinetics do not require connectivity of PSII units (Sipka *et al.* 2021). (*3*) Using fast Chl *a* fluorescence induction (OJIP) kinetics in the absence of DCMU, it has been thoroughly documented that the so-called photochemical phase (Delosme 1967), the O-to-J step, does not reach the maximum (P) level even at very high light intensities – when in the 2-ms window of the O–J phase each PSII receives dozens of excitations (Neubauer and Schreiber 1987, Lazár and Pospíšil 1999, Schansker *et al.* 2011). This is difficult to explain using the Q_A model – and in fact different complementary mechanisms, such as conformational changes (Moise and Moya 2004, Schansker *et al.* 2014) and photoelectrochemical effects (Vredenberg and Prasil 2013, Vredenberg 2015), were invoked. On the other hand, these data can easily be reconciled by taking into account the observed waiting times of several hundred microseconds to 1–2 ms, affecting F_v (Magyar *et al.* 2018, Sipka *et al.* 2021), and the competing event, the Q_A-to-Q_B electron transfer (Shlyk-Kerner *et al.* 2006), which reopens PSII and thus hinders the rise, leading to the J-to-I transition.

The $PSII_C$-to-$PSII_L$ transition and the waiting times were proposed to originate from conformational changes and dielectric relaxation processes, due to the formation of stationary and transient local electric fields in the vicinity of the RCs; contributions from thermal transients, associated with charge recombination and excitation energy dissipation were also considered (Sipka *et al.* 2021). Nevertheless, the nature and physical mechanisms of these processes are not well understood and require further, systematic investigations. It is plausible to assume – and also indicated by the observed variations of $\Delta\tau_{1/2}$ from batch to batch of isolated detergent-solubilized cyanobacterial PSII core complexes (PSII CCs) as well as between whole cyanobacterial cells and thylakoid membrane preparations and at different temperatures – that these processes depend on the physicochemical environment of the RC. In particular, they might be sensitive to the hydration state of the sample, the presence of different ions, conformational mobility of different protein residues, and the lipid content and composition of the preparations. Our first target in this series of investigations is the lipidic matrix of PSII.

The lipid membrane of thylakoids of cyanobacteria, algae, and plants serves as a matrix for the photosynthetic pigment–protein complexes (Nelson and Ben-Shem 2004); it prevents the free diffusion of ions across the bilayer, thus facilitating the formation of a transmembrane electrochemical potential gradient, which is utilized during the synthesis of ATP (Dimroth *et al.* 2000). Thylakoid membranes (TMs) possess a unique composition of lipids with a majority of glycolipids, monogalactosyldiacylglycerol (MGDG), digalactosyldiacylglycerol (DGDG), and sulfoquinovosyldiacylglycerol (SQDG); they also contain, as minor lipid constituents, the phospholipid phosphatidylglycerol (PG) molecules. MGDG plays a role in the formation of chloroplast membranes (Jarvis *et al.* 2000) and, as a non-bilayer lipid, in the photoprotection of the photosynthetic machinery *via* warranting the activity of the xanthophyll cycle (Siefermann and Yamamoto 1975, Yamamoto and Higashi 1978, Latowski *et al.* 2004, Dlouhý *et al.* 2020, Goss and Latowski 2020). DGDG might be responsible for the development and stabilization of the membrane (Lee 2000) and the OEC (Sakurai *et al.* 2007) and is required for the thermal stability of PSII (Reifarth *et al.* 1997) as well as of PSI (Krumova *et al.* 2010). SQDG affects the electron transfer from OEC to Y_Z on the donor side of PSII (Minoda *et al.* 2003). Regarding PG, a series of reports demonstrated its function in dimerization of PSII (Kruse *et al.* 2000) and the electron transfer at the Q_B-binding site (Gombos *et al.* 2002, Leng *et al.* 2008).

The lipid compositions of thylakoid membranes prepared from spinach and *T. vulcanus* cells and of the PSII dimer complex of *T. vulcanus* were revealed by Sakurai *et al.* (2006); these samples, respectively, contained the following lipid species: MGDG accounted for about ~ 40, ~ 44, and 30% of the total lipids; DGDG was ~ 32, ~ 26, and 21%; SQDG ~ 15, ~ 25, and 20%; and PG occupied 13, 6, and 29% of the total lipids. They estimated the numbers of the lipid molecules bound in PSII from the Chl and Pheo content and obtained 27 and 8 lipid molecules per monomer of *T. vulcanus* and spinach, respectively. The lipid composition of thylakoid membranes and corresponding PSII complexes were quite different, especially since the relative content of PG was much higher in the PSII complexes than that in the thylakoid membranes (Sakurai *et al.* 2006). The crystal structure of PSII of *T. vulcanus* at a resolution of 1.9 Å revealed more than 20 lipids per monomer, namely, six MGDG, five DGDG, four SQDG, and five PG together with 15/14 detergent molecules per D_1/D_2 monomers (Umena *et al.* 2011).

Upon purification and isolation of the RCs and core complexes, some of the native membrane lipids are replaced by detergent molecules. Several studies have shown that photosynthetic pigment–protein complexes are sensitive to different detergents and detergent concentrations (Heinemeyer *et al.* 2004, Akhtar *et al.* 2015). In particular, detergent solubilization of the PSII RC complex has been shown to perturb the energy transfer pathway from the accessory Chl *a* (Tang *et al.* 1991). In bacterial RC, it was found that the electron transfer steps (Tiede *et al.* 1996, Lavergne *et al.* 1999) and the $P^+Q_A^- \rightarrow PQ_A$ charge recombination (Sebban and Wraight 1989) were considerably faster in lipid membrane than in the detergent-solubilized sample.

These observations justify our aims to investigate the possible effects of the lipidic environment on the origin of the rate-limiting steps in PSII. Here we performed measurements with double-flash excitations with variable $\Delta\tau$ waiting times between them using *T. vulcanus* PSII CCs in solution with or without added detergent and embedded into different liposomes, as well as in pea thylakoid membranes and whole cyanobacterial cells. We found that – while steady-state and time-resolved spectroscopic

data revealed only minor alterations between different samples – the $\Delta\tau_{1/2}$ values were considerably shorter when the RC complexes were located in the TMs or embedded in TM liposomes than those in detergent or non-TM liposomes.

Materials and methods

Source material: *Thermosynechococcus vulcanus*, a thermophilic cyanobacterial strain isolated from a hot spring in Yunomine, Japan (Koike and Inoue 1983), was grown as a batch culture. Pea (*Pisum sativum*) plants were grown in a greenhouse at 22°C under natural light conditions.

Growth conditions: *T. vulcanus* cells were grown photoautotrophically in a BG11 medium (pH 7.0) at 50°C under continuous illumination with a white fluorescent lamp at a photon flux density of 50–100 μmol m^{-2} s^{-1} (Shen *et al.* 2011). Cultures were aerated on a gyratory shaker operating at 100 rpm.

Sample preparation: Isolation of thylakoid membranes from fresh pea (*P. sativum*) leaves was performed essentially as described earlier (Chylla *et al.* 1987), with minor modifications. Briefly, deveined leaves were homogenized in a buffer containing 20 mM Tricine (pH 8.0), 0.4 M NaCl, and 2 mM $MgCl_2$, filtered through a nylon mesh, and the supernatant was centrifuged for 7 min at 6,000 × *g*. The pellet was resuspended in a hypotonic buffer containing 20 mM Tricine (pH 8.0), 0.15 M NaCl, and 5 mM $MgCl_2$, followed by centrifugation for 7 min at 6,000 × *g*. The pellet was finally resuspended in the resuspension buffer containing 20 mM MES (pH 6.5), 0.4 M sucrose, 5 mM $MgCl_2$, and 15 mM NaCl, and stored in liquid nitrogen at a Chl concentration of 2–3 mg mL^{-1}.

PSII CCs of *T. vulcanus* were isolated as described earlier (Shen and Inoue 1993, Shen and Kamiya 2000, Shen *et al.* 2011, Kawakami and Shen 2018). Essentially, the final steps of the PSII CC purification were the elution of the column containing crude PSII with a column buffer [30 mM MES-NaOH (pH 6.0), 3 mM $CaCl_2$, 0.03% β-DDM, and 1 M NaCl] with a linear gradient of 170–300 mM NaCl; then centrifugation of the PSII CC after the addition of 13% PEG 1,450 to precipitate and concentrate the sample and dilution in a buffer containing 30 mM MES–NaOH (pH 6.0), 20 mM NaCl, and 3 mM $CaCl_2$. PSII dimers were then suspended in the same buffer and stored in liquid nitrogen until use. For all the experiments, the isolated PSII CCs were diluted in a reaction buffer containing 5% glycerol, 20 mM MES (pH 6.0), 20 mM NaCl, 3 mM $CaCl_2$; in some experiments, the reaction medium was complemented with 0.03% β-DDM.

Proteoliposome preparation: Liposomes were prepared with three different types of lipid mixtures [PC from soybean, PC and PE (80:20) and plant thylakoid lipid mixture of 45% (w/v) MGDG, 30% DGDG, 15% PG, and 10% SQDG]. The organic solvent (chloroform:methanol, 1:1) from the lipid mixture was slowly dried in a vacuum rotatory evaporator to form a thin film of lipids on the wall of a round-bottom glass vial. After completely drying the solvent, the lipid film was hydrated with the PSII buffer to a total lipid concentration of 5 mg mL^{-1}. The suspension was vortexed for approximately 40–50 min and subsequently subjected to ten freeze–thaw cycles. Large unilamellar vesicles were formed by extruding the suspension through a 100-nm pore membrane (*Mini-Extruder*, *Avanti Polar Lipids*, Birmingham, UK). The liposomes were then destabilized by adding 0.05% detergent (β-DDM) and the isolated solubilized PSII CCs were added dropwise to the liposome suspension to a final molar lipid:protein ratio of 300:1 (assuming 35 Chls per monomeric PSII) while agitating continuously. The mixture was then incubated at room temperature (RT) for 20 min in the dark. The detergent was then removed by repeated incubation of the sample with absorbent beads (*Bio-Beads SM2*, *Bio-Rad*, USA). The average diameter of the reconstituted PSII membranes was 0.5–0.7 μm as determined by dynamic light scattering (*Zetasizer Nano ZS*, Malvern, UK).

Absorption and circular dichroism spectroscopy: Absorption and circular dichroism (CD) spectra in the range of 350–750 nm were recorded at RT with a *Thermo Evolution 500* dual-beam spectrophotometer (Cambridge, UK) and a *Jasco J-815* spectropolarimeter (Pfungstadt, Germany), respectively. The samples were diluted in 20 mM Tricine buffer (pH 7.5) to an absorbance of 1.0 at the red maximum. The measurements were performed in a standard glass cell of 1-cm optical path length with 1-nm (absorption) or 2-nm (CD) spectral bandwidth.

Fluorescence yield measurements: Relative fluorescence yields were measured using a *PAM* (Pulse Amplitude Modulation) *101* fluorometer (*Walz*, Effeltrich, Germany). The frequency of the modulated measuring light (low intensity, nonactinic) was 1.6 kHz. Variable fluorescence was induced by STSFs (Xe flashes, *Excelitas LS-1130-3 Flashpac with FX-1163 Flashtube* with reflector, Wiesbaden, Germany) of 1.5-μs duration at half-peak intensity. The sample was placed at the sample holder of a thermoluminescence apparatus to control the temperature. The timing of the flashes was controlled by using a home-designed programmable digital pulse generator. The kinetic traces were recorded by using a *National Instruments* data acquisition device (*DAQ 6001*, Austin, USA) *via* custom-designed *LabVIEW* software. For Chl *a* fluorescence transient measurements, the Chl concentration of the thylakoid membranes was diluted to ~ 20 μg mL^{-1} in the resuspension buffer; and that of the PSII CC to ~ 5 μg mL^{-1} in the reaction buffer or when embedded into lipids in glycerol-free reaction buffer. DCMU was dissolved in dimethyl sulfoxide and added to all samples immediately before the fluorescence measurements at a final concentration of 40 μM (the final dimethyl sulfoxide concentration did not exceed 1%). Before the measurements, the samples were dark-adapted for 5 min at RT, then cooled to 5°C, and then temperature adapted for 5 more min.

Steady-state fluorescence spectroscopy: Fluorescence emission spectra at 77 K were recorded with a *Fluorolog 3* double-monochromator spectrofluorometer (*Horiba Jobin-Yvon*, USA). An aliquot of 40 µL of PSII CC solution with the absorbance of 0.3 at the red maximum was evenly placed onto a *Whatman GF/C* glass microfiber filter and immersed in liquid nitrogen in a Dewar glass vessel. Spectra were recorded in the range of 600–800 nm with 440-nm excitation light and 3-nm excitation and emission spectral bandwidths. The measurements were performed with 1-nm increments and 1-s integration time.

RT fluorescence spectra were recorded with an *FP-8500* spectrofluorometer (*Jasco*, Japan). The samples were diluted to the absorbance of 0.01 at the red maximum and placed in a 1-cm quartz cell. Spectra in the range of 620–780 nm were recorded with an excitation wavelength of 440 nm and excitation and emission bandwidths of 5 nm.

Time-resolved fluorescence spectroscopy: Picosecond time-resolved fluorescence measurements were performed using a time-correlated single-photon counting instrument (*FluoTime 200*/*PicoHarp 300* spectrometer, *PicoQuant*, Berlin, Germany) described earlier (Akhtar *et al.* 2016). Excitation was provided by *Fianium WhiteLase Micro* (*NKT Photonics*, Southampton, UK) supercontinuum laser, generating white-light pulses with a repetition rate of 20 MHz. Excitation wavelengths of 440 or 632 nm were selected using bandpass filters. The fluorescence decays were recorded at wavelengths of 664–744 nm with 8-nm steps. The total instrument response (IRF) measured using 1% Ludox as scattering solution has a width of 40 ps. Fluorescence decays collected at different detection wavelengths were analysed by a global lifetime and IRF reconvolution using analysis routines written in *MATLAB*.

The samples were diluted to an absorbance of 0.03 at excitation wavelength in a 1-mm flow cell. To keep the RCs in an open state, the reaction buffer was supplemented with 25 µM dichlorophenolindophenol and 0.5 mM ferricyanide and continuously circulated at a flow rate of 4 mL min^{-1} to avoid the repeated excitation of the RC. Measurements with closed preilluminated RCs, close to the F_m state, were performed by adding 20 µM DCMU to the reaction buffer and circulating the sample at a lower flow rate or using an additional background illumination source.

Results and discussion

Chlorophyll *a* fluorescence – determination of $\Delta\tau_{1/2}$: Upon illumination of DCMU-treated, dark-adapted *T. vulcanus* PSII CC by a train of double STSFs with different waiting times ($\Delta\tau$) between the two consecutive flashes, a stepwise rise of the Chl *a* fluorescence yield was observed (the transients recorded at RT, and the effect of $\Delta\tau$, are illustrated in Fig. 1S, *supplement*). Comparable data were obtained earlier in *T. vulcanus* PSII CC, whole cyanobacterial cells, and spinach thylakoid membranes at different temperatures (Magyar *et al.* 2018, Sipka *et al.* 2019). Excitation of PSII CCs with an STSF in the presence of DCMU leads to the reduction of Q_A and no further stable charge separation can be obtained by additional excitations. However, by using a second STSF, the fluorescence level increases, but only after a sufficiently long $\Delta\tau$ dark waiting time between the two STSFs (Magyar *et al.* 2018). Here, after a few double-flash excitations, we applied MTSFs to convincingly reach F_m. It is important to emphasize that identical fluorescence levels were obtained with a single STSF and by simultaneously firing two STSFs (data not shown), confirming that our single-turnover exciting flashes are saturating. As shown in Fig. 1S, upon applying a 10-µs waiting time between the two STSFs, no sizeable increase could be detected in the fluorescence level, while the F_1-to-F_2 increment was maximal with $\Delta\tau$ longer than 10 ms.

To test the effect of the lipidic environment on the rate-limiting step, we performed our double-STSF measurements on *T. vulcanus* PSII CCs in different liposomes and compared them with PSII CC of the same batches in solution. In separate experiments, we confirmed that $\Delta\tau_{1/2}$ was essentially the same in the presence (above CMC) and absence (300–400× dilution depending on the PSII CC batch concentration) of additional detergent β-DDM. Indeed, the data showed no significant difference in the $\Delta\tau_{1/2}$ values, which, at 5°C, were ~ 1.5 ms without added detergent and ~ 1.2 ms with 0.03% β-DDM (Fig. 1*A*; Table 1S, *supplement*). This might be suggesting that the detergent micelle formed around the PSII CC does not influence the rate-limiting step. We estimated the half-rise time ($\Delta\tau_{1/2}$) of the F_1-to-F_2 fluorescence increment from a logistic function fit of the dependence of the fluorescence increment on $\Delta\tau$ (Fig. 1). Earlier we used a simpler exponential fit to determine $\Delta\tau_{1/2}$ (Magyar *et al.*

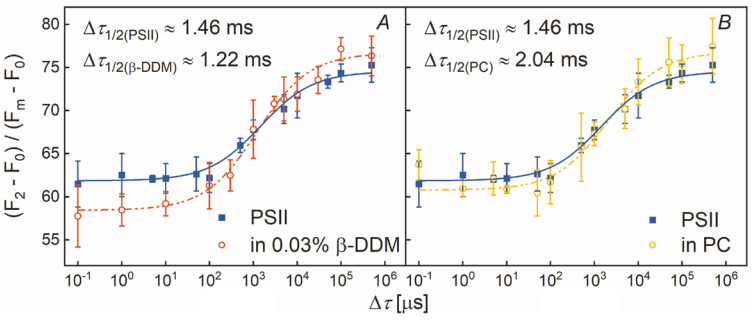

Fig. 1. Dependence of the F_1-to-F_2 increment on the waiting time ($\Delta\tau$), between the first and second STSFs, of PSII CC of *Thermosynechococcus vulcanus* in solution (*blue*) (*A*,*B*), and in buffer containing 0.03% β-DDM (*red*) (*A*), and embedded into PC liposomes (*yellow*) (*B*) – at 5°C in the presence of 40 µM DCMU. *Continuous lines* represent logistic-function fits of the data points, which represent mean values ± SD (n = 3–5). The magnitude of the increment at each $\Delta\tau$ was determined by measuring the F_2 fluorescence level elicited by the second STSF delivered after $\Delta\tau$ waiting time for the first flash.

2018); however, a more accurate model is warranted to judge the differences in half-rise times between experiments.

PSII CC in PC liposomes showed a $\Delta\tau_{1/2}$ of ~ 2 ms at 5°C and ~ 0.5 ms at RT (n = 3–5, for different data points). These values were comparable to the ones measured from the matching PSII CC batches in solution (without added detergent) – $\Delta t_{1/2}$ of ~ 1.5 ms at 5°C and ~ 1 ms at RT (Fig. 1*B*, Table 1S) – indicating that PC has no significant effect on the rate limitation. Similar data were obtained with PSII CC embedded in the PC-PE liposome (Table 1S).

In contrast, when PSII CCs were reconstituted into TM lipids, a substantial difference could be discerned. The half-rise time decreased to ~ 0.2 ms at 5°C, which was much faster than that of the same PSII CCs in solution (Fig. 2*A*). To see if this acceleration in thylakoid lipids is a more general phenomenon, we performed experiments on pea thylakoid membranes (Table 1S) and *T. vulcanus* cells (Fig. 2*B*). We found similar $\Delta\tau_{1/2}$ values in different batches of cells and isolated pea TMs (Table 1S). We used two different *T. vulcanus* cell cultures, one was grown by shaking and measured with *PAM 101*, the other one was cultivated by bubbling with air supplemented with 1–5% CO_2 and measured with *DUAL PAM* Chl *a* fluorometer (Fig. 2*B* and Table 1S, respectively). These observations indicate that one or more lipids of the TM lipid mixture influence the rate limitation.

Absorption and CD spectra of PSII in detergent and lipid environment: CD spectroscopy is a highly sensitive tool to detect even minute changes in the excitonic interactions of pigment–protein complexes (Garab and van Amerongen 2009, Akhtar *et al.* 2016). We recorded absorption and CD spectra of PSII CCs in solution and compared them with reconstituted membranes of PSII (Fig. 3). The absorption spectra (Fig. 3*A*) are dominated by Chl *a*, with absorption maxima at 436 and 674 nm in the Soret and the red region, respectively. Carotenoid (Car) absorption is visible in the wavelength range from 450 to 500 nm. In the red region, the CD spectra (Fig. 3*B*) are characterized by a positive–negative band pair with maxima at 672 and 681 nm, associated with the Q_y exciton states of Chl *a*. A shoulder at 686 nm likely reflects the excitonic interactions between Chls P_{D1} and P_{D2} in the RC, whereas the 681-nm peak primarily originates from the core antenna (Hinz 1985, Alfonso *et al.* 1994). In the blue region, the spectra display more bands, owing to the multitude of Chl and Car transitions. The 505-nm band is associated with β-carotenes of the RC.

The CD spectrum of PSII CCs incorporated into proteoliposomes with native thylakoid lipids was essentially the same as the spectrum of solubilized PSII, indicating that the lipid/detergent environment does not exert any significant change in the Chl excitonic energies and interactions. In contrast, the CD spectrum of peripheral antenna complexes (LHCII) does show specific changes caused by the lipid/detergent environment (Akhtar *et al.* 2015). It should be pointed out that the PSII CC proteoliposomes used here had approximately equal amounts of lipid and protein (per mass unit), whereas the protein content of granal thylakoid membranes is significantly higher (Duchêne and Siegenthaler 2000, Haferkamp *et al.* 2010). Hence, we do not expect aggregation or dense packing of PSII CCs in the proteoliposomes beyond what natively occurs in thylakoid membranes.

Fluorescence emission spectra: Fluorescence emission spectra of PSII CCs in solution and liposomes were recorded at RT (Fig. 2S, *supplement*) and 77 K (Fig. 4). No differences were observed in the fluorescence emission at RT. The 77 K fluorescence emission spectrum of the PSII CCs exhibited an emission maximum at 694 nm, originating from a red-shifted Chl in CP47, and a lower-intensity shoulder at 686 nm (Andrizhiyevskaya *et al.* 2005, Sipka *et al.* 2021). Upon reconstitution into lipid membranes, the peak ratios changed – the 686-nm peak from the bulk antenna Chls became the dominant one, whereas the CP47 emission at 694 nm was lower. Similar changes, although to a much lesser extent, were observed in the fluorescence emission peak ratios of native PSII-enriched membranes upon fusing with liposomes (Haferkamp *et al.* 2010). Interestingly, the values of the peak ratios of the reconstituted PSII CC membranes were comparable to those in native thylakoid membranes and whole cells of *T. vulcanus* (Table 2S, *supplement*). The peak ratio at 77 K depends on the dynamic balance of excitation energy trapping by the red-shifted states in CP47 *vs.* trapping in the RC (Shibata *et al.* 2013). A change in the peak ratio induced by the environment could indicate conformational instability of the complexes. The PSII core antenna proteins have been shown to undergo structural changes when extracted from their native environment that

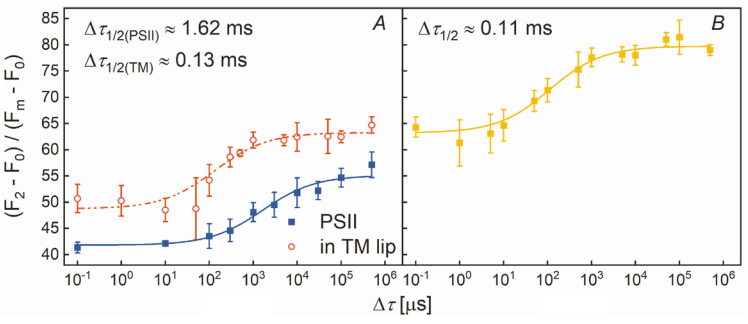

Fig. 2. Dependence of the F_1-to-F_2 increment on the waiting time ($\Delta\tau$), between the first and second STSFs, of *Thermosynechococcus vulcanus* PSII CC in solution (*blue*) and embedded into thylakoid lipids (TM lip, *red*) at 5°C (*A*), and of *T. vulcanus* cells (*yellow*) at RT (*B*) – in the presence of 40 μM DCMU. *Continuous lines* represent logistic-function fits of the data points, which represent mean values ± SD (n = 3–5). The magnitude of the increment at each $\Delta\tau$ was determined by measuring the F_2 fluorescence level elicited by the second STSF delivered after $\Delta\tau$ waiting time for the first flash.

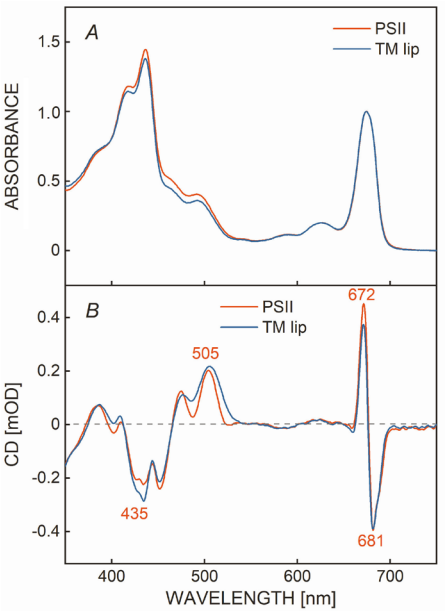

Fig. 3. Absorption (*A*) and CD (*B*) spectra of *Thermosynechococcus vulcanus* PSII CC in solution (PSII) and embedded into TM-lipid membranes. The spectra are normalized to the unity absorbance of each sample at 675 nm.

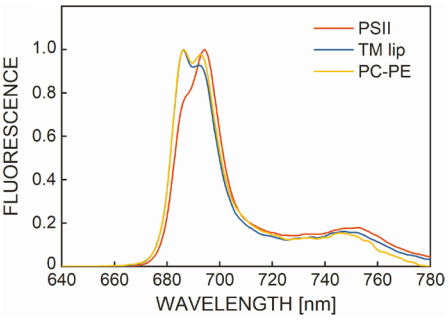

Fig. 4. 77 K steady-state fluorescence emission spectra of *Thermosynechococcus vulcanus* PSII CCs in solution (PSII) and embedded into different lipid membranes (TM lipid and PC-PE); excitation wavelength, 440 nm. The spectra are normalized to the maximum fluorescence intensities and are corrected for the detector spectral sensitivity.

affects the Chl exciton energies and possibly excitation dynamics (Sirohiwal *et al.* 2021). Kansy *et al.* (2014) also reported a change in the amplitude of the 694-nm emission in plant PSII CCs upon the addition of positively charged lipids. They interpreted this change as resulting from the partial detachment of CP43, which exposes CP47 to the polar environment and alters the excited-state energy of the red-shifted Chls. However, these changes are not related to the lipid-dependent variations of $\Delta\tau_{1/2}$ since the changes were not specific to TM lipids.

Time-resolved fluorescence spectroscopy: To check possible differences in the excitation dynamics of PSII in solution and reconstituted lipid membranes, we performed time-resolved fluorescence spectroscopy with picosecond resolution at RT under conditions close to $PSII_O$ (F_0) and $PSII_L$ (F_m). The corresponding fluorescence decay kinetics are compared in Fig. 3S (*supplement*). In all cases, the fluorescence shows rapid decay for PSII CCs with open RCs compared to closed RCs. Global lifetime analysis was applied to the fluorescence decay kinetics recorded at wavelengths 664–744 nm over a 4-ns window. The resulting decay-associated emission spectra (DAES) are shown in Fig. 5 and Fig. 4S (*supplement*). Three decay components were sufficient to describe the kinetics of PSII with open RC. The majority of the excitations (> 97%) decayed with two lifetimes – around 50 and 300 ps (Miloslavina *et al.* 2006, van der Weij-de Wit *et al.* 2011, Sipka *et al.* 2021). A low-amplitude (2–3%) nanosecond decay component may originate from a small fraction of closed-state PSII. When the complexes were incorporated in lipid membranes, both lifetimes increased by about 10%, as did the relative amplitude of the slower decay component, so that the average lifetime increased from about 100 to 150 ps. These changes may indicate a slight alteration of the kinetics of excitation energy transfer to the RC induced by the lipid environment. Alternatively, it is also possible that some of the PSII complexes in proteoliposomes assume a closed state under the measurement conditions. In support of the latter, we observe that the relative amplitude of the nanosecond component also increased – from 1 to 3%. As mentioned above, one possible explanation for the changes in the stationary fluorescence emission spectra at 77 K could be the partial dissociation or functional detachment of CP43, induced by charged lipids (Kansy *et al.* 2014). Any such decoupling

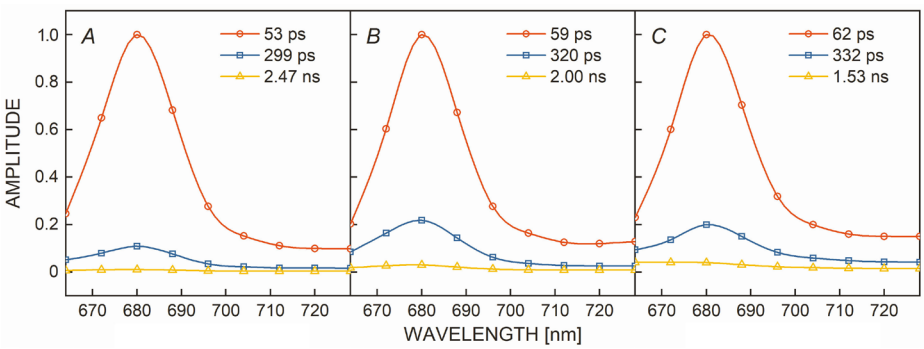

Fig. 5. Decay-associated fluorescence emission spectra of *Thermosynechococcus vulcanus* PSII CC in solution (*A*) and embedded into TM lipid (*B*) and PC-PE membranes (*C*) – in F_0 state; the spectra are obtained by global lifetime analysis of the fluorescence decays recorded at RT with 632-nm excitation.

should be detectable in the fluorescence kinetics, which should acquire a long-lived component with a lifetime of 2–4 ns (the excitation lifetime of the uncoupled antenna). Based on the small amplitude of the 2-ns component (< 5%), we conclude that in our conditions, there is no sizeable decoupling of CP43 from the RC.

A more complex dynamics is characteristic for pre-illuminated PSII with closed RCs (Fig. 4S) with several decay lifetimes from 80 ps to 4 ns and an average lifetime of ~ 0.9 ns (Szczepaniak *et al.* 2009, Sipka *et al.* 2021). Under these conditions, the lipid/detergent environment did not incur readily discernible changes in the fluorescence kinetics. This can be taken as an indication that the kinetics of charge recombination in the light-adapted closed state of the RC is not significantly influenced by the lipid environment.

Conclusion and perspectives: In this work, we investigated the question of whether and how the lipid matrix of PSII RCs affects the dark-to-light transition of this photosystem. To this end, we studied the waiting time ($\Delta\tau$)-dependent rise of the Chl *a* fluorescence of different closed (DCMU-treated) PSII-containing samples. We found no significant difference in the $\Delta\tau_{1/2}$ half-waiting times between PSII CC samples with 0.03% added β-DDM and those containing only residual amounts of detergent. Also, non-native lipids, such as PC or a mixture of PC and PE, exerted no significant effect on $\Delta\tau_{1/2}$. We emphasize that a detergent shell and lipid shells surrounding the complexes have no sizeable effect on the $\Delta\tau_{1/2}$ values indicating that the $\Delta\tau$ waiting time is essentially insensitive to the lipidic or detergent environment of the core complexes. This is in line with the proposed origin of $\Delta\tau$ from dielectric relaxation processes following variations in the local electric fields inside the RC (Sipka *et al.* 2021). On the other hand, $\Delta\tau_{1/2}$ was considerably shorter in all samples, which either retained the original lipid environment of PSII (in TMs and whole cells) or in which the missing lipids were replenished with TM lipids (the case of PSII CCs embedded in liposomes formed by TM lipids). Further experiments are required to identify the lipid molecule(s) which appeared to restore the $\Delta\tau_{1/2}$ that is characteristic of TMs and to clarify the role(s) of the different lipid molecules which participate in the dynamic dark-to-light transition of PSII. In this respect, studying lipid mutants, or samples with markedly different lipid compositions, with Chl *a* fluorescence transients using double STSFs, would be of high interest. Nevertheless, the presently available data clearly show that the underlying process(es) depend(s) on the lipid matrix of the PSII RC.

Lipids, in general, are known to increase the structural flexibility of proteins and may act as lubricants for protein motions (*cf.* Duncan *et al.* 2016). Hence, our data underscore the significance of the structural flexibility of PSII and minute light-induced conformational transitions in $PSII_C$ – in good agreement with our earlier data and conclusions (Magyar *et al.* 2018, Sipka *et al.* 2021). It remains to be elucidated if the role of lipids is to be found in accelerating the dielectric relaxation processes of PSII CCs or they act *via* facilitating the transduction of the heat packages, associated with the charge recombination events, to the protein matrix or the medium – these physical mechanisms have been proposed to be involved in the $PSII_C$-to-$PSII_L$ transition (Magyar *et al.* 2018, Sipka *et al.* 2021).

References

Akhtar P., Dorogi M., Pawlak K. *et al.*: Pigment interactions in light-harvesting complex II in different molecular environments. – J. Biol. Chem. **290**: 4877-4886, 2015.

Akhtar P., Lingvay M., Kiss T. *et al.*: Excitation energy transfer between Light-harvesting complex II and Photosystem I in reconstituted membranes. – BBA-Bioenergetics **1857**: 462-472, 2016.

Alfonso M., Montoya G., Cases R. *et al.*: Core antenna complexes, Cp43 and Cp47, of higher plant photosystem II. Spectral properties, pigment stoichiometry, and amino acid composition. – Biochemistry-US **33**: 10494-10500, 1994.

Andrizhiyevskaya E.G., Chojnicka A., Bautista J.A. *et al.*: Origin of the F685 and F695 fluorescence in Photosystem II. – Photosynth. Res. **84**: 173-180, 2005.

Brettel K., Schlodder E., Witt H.T.: Nanosecond reduction kinetics of photooxidized chlorophyll-a_{II} (P-680) in single flashes as a probe for the electron pathway, H+-release and charge accumulation in the O_2-evolving complex. – BBA-Bioenergetics **766**: 403-415, 1984.

Cardona T., Sedoud A., Cox N., Rutherford A.W.: Charge separation in Photosystem II: A comparative and evolutionary overview. – BBA-Bioenergetics **1817**: 26-43, 2012.

Chylla R.A., Garab G., Whitmarsh J.: Evidence for slow turnover in a fraction of Photosystem II complexes in thylakoid membranes. – BBA-Bioenergetics **894**: 562-571, 1987.

Delosme R.: [Study of the induction of fluorescence in green algae and chloroplasts at the onset of an intense illumination.] – BBA-Bioenergetics **143**: 108-128, 1967. [In French]

Dimroth P., Kaim G., Matthey U.: Crucial role of the membrane potential for ATP synthesis by F_1F_o ATP synthases. – J. Exp. Biol. **203**: 51-59, 2000.

Dlouhý O., Kurasová I., Karlický V. *et al.*: Modulation of non-bilayer lipid phases and the structure and functions of thylakoid membranes: effects on the water-soluble enzyme violaxanthin de-epoxidase. – Sci. Rep.-UK **10**: 11959, 2020.

Duchêne S., Siegenthaler P.-A.: Do glycerolipids display lateral heterogeneity in the thylakoid membrane? – Lipids **35**: 739-744, 2000.

Duncan A.L., Robinson A.J., Walker J.E.: Cardiolipin binds selectively but transiently to conserved lysine residues in the rotor of metazoan ATP synthases. – P. Natl. Acad. Sci. USA **113**: 8687-8692, 2016.

France L.L., Geacintov N.E., Breton J., Valkunas L.: The dependence of the degrees of sigmoidicities of fluorescence induction curves in spinach chloroplasts on the duration of actinic pulses in pump-probe experiments. – BBA-Bioenergetics **1101**: 105-119, 1992.

Garab G., van Amerongen H.: Linear dichroism and circular dichroism in photosynthesis research. – Photosynth. Res. **101**: 135-146, 2009.

Gombos Z., Várkonyi Z., Hagio M. *et al.*: Phosphatidylglycerol requirement for the function of electron acceptor plastoquinone Q_B in the photosystem II reaction center. – Biochemistry-US **41**: 3796-3802, 2002.

Goss R., Latowski D.: Lipid dependence of xanthophyll cycling in higher plants and algae. – Front. Plant Sci. **11**: 455, 2020.

Haferkamp S., Haase W., Pascal A.A. *et al.*: Efficient light

harvesting by photosytem II requires an optimized protein packing density in grana thylakoids. – J. Biol. Chem. **285**: 17020-17028, 2010.

Hansson O., Wydrzynski T.: Current perceptions of Photosystem II. – Photosynth. Res. **23**: 131-162, 1990.

Heinemeyer J., Eubel H., Wehmhöner D. *et al.*: Proteomic approach to characterize the supramolecular organization of photosystems in higher plants. – Phytochemistry **65**: 1683-1692, 2004.

Hinz U.G.: Isolation of the photosystem II reaction center complex from barley. Characterization by circular dichroism spectroscopy and amino acid sequencing. – Carlsberg Res. Commun. **50**: 285-298, 1985.

Horton P., Ruban A.: Molecular design of the photosystem II light-harvesting antenna: photosynthesis and photoprotection. – J. Exp. Bot. **56**: 365-373, 2005.

Jarvis P., Dörmann P., Peto C.A. *et al.*: Galactolipid deficiency and abnormal chloroplast development in the *Arabidopsis MGD synthase 1* mutant. – P. Natl. Acad. Sci. USA **97**: 8175-8179, 2000.

Joliot P., Joliot A.: Comparative study of the fluorescence yield and of the C550 absorption change at room temperature. – BBA-Bioenergetics **546**: 93-105, 1979.

Kalaji H.M., Schansker G., Ladle R.J. *et al.*: Frequently asked questions about *in vivo* chlorophyll fluorescence: practical issues. – Photosynth. Res. **122**: 121-158, 2014.

Kansy M., Wilhelm C., Goss R.: Influence of thylakoid membrane lipids on the structure and function of the plant photosystem II core complex. – Planta **240**: 781-796, 2014.

Kawakami K., Shen J.R.: Purification of fully active and crystallizable photosystem II from thermophilic cyanobacteria. – Method. Enzymol. **613**: 1-16, 2018.

Koike H., Inoue Y.: Preparation of oxygen-evolving photosystem II particles from a thermophilic blue-green alga. – In: Inoue Y., Crofts A.R., Govindjee *et al.* (ed.): The Oxygen Evolving System of Photosynthesis. Pp. 257-263. Academic Press, Tokyo 1983.

Krumova S.B., Laptenok S.P., Kovács L. *et al.*: Digalactosyldiacylglycerol-deficiency lowers the thermal stability of thylakoid membranes. – Photosynth. Res. **105**: 229-242, 2010.

Kruse O., Hankamer B., Konczak C. *et al.*: Phosphatidylglycerol is involved in the dimerization of photosystem II. – J. Biol. Chem. **275**: 6509-6514, 2000.

Laisk A., Oja V.: Variable fluorescence of closed photochemical reaction centers. – Photosynth. Res. **143**: 335-346, 2020.

Latowski D., Åkerlund H.E., Strzalka K.: Violaxanthin de-epoxidase, the xanthophyll cycle enzyme, requires lipid inverted hexagonal structures for its activity. – Biochemistry-US **43**: 4417-4420, 2004.

Lavergne J., Matthews C., Ginet N.: Electron and proton transfer on the acceptor side of the reaction center in chromatophores of *Rhodobacter capsulatus*: Evidence for direct protonation of the semiquinone state of Q_B. – Biochemistry-US **38**: 4542-4552, 1999.

Lavergne J., Trissl H.W.: Theory of fluorescence induction in photosystem II: derivation of analytical expressions in a model including exciton-radical-pair equilibrium and restricted energy transfer between photosynthetic units. – Biophys. J. **68**: 2474-2492, 1995.

Lazár D., Pospíšil P.: Mathematical simulation of chlorophyll *a* fluorescence rise measured with 3-(3',4'-dichlorophenyl)-1,1-dimethylurea-treated barley leaves at room and high temperatures. – Eur. Biophys. J. **28**: 468-477, 1999.

Lee A.G.: Membrane lipids: It's only a phase. – Curr. Biol. **10**: R377-R380, 2000.

Leng J., Sakurai I., Wada H., Shen J.-R.: Effects of phospholipase and lipase treatments on photosystem II core dimer from a thermophilic cyanobacterium. – Photosynth. Res. **98**: 469-478, 2008.

Magyar M., Sipka G., Kovács L. *et al.*: Rate-limiting steps in the dark-to-light transition of Photosystem II – revealed by chlorophyll-*a* fluorescence induction. – Sci. Rep.-UK **8**: 2755, 2018.

Miloslavina Y., Szczepaniak M., Müller M.G. *et al.*: Charge separation kinetics in intact photosystem II core particles is trap-limited. A picosecond fluorescence study. – Biochemistry-US **45**: 2436-2442, 2006.

Minoda A., Sonoike K., Okada K. *et al.*: Decrease in the efficiency of the electron donation to tyrosine Z of photosystem II in an SQDG-deficient mutant of *Chlamydomonas*. – FEBS Lett. **553**: 109-112, 2003.

Moise N., Moya I.: Correlation between lifetime heterogeneity and kinetics heterogeneity during chlorophyll fluorescence induction in leaves: 1. Mono-frequency phase and modulation analysis reveals a conformational change of a PSII pigment complex during the IP thermal phase. – BBA-Bioenergetics **1657**: 33-46, 2004.

Nelson N., Ben-Shem A.: The complex architecture of oxygenic photosynthesis. – Nat. Rev. Mol. Cell Biol. **5**: 971-982, 2004.

Neubauer C., Schreiber U.: The polyphasic rise of chlorophyll fluorescence upon onset of strong continuous illumination: I. Saturation characteristics and partial control by the photosystem II acceptor side. – Z. Naturforsch. C **42**: 1246-1254, 1987.

Nuijs A.M., van Gorkom H.J., Plijter J.J., Duysens L.N.M.: Primary-charge separation and excitation of chlorophyll a in photosystem II particles from spinach as studied by picosecond absorbance-difference spectroscopy. – BBA-Bioenergetics **848**: 167-175, 1986.

Oja V., Laisk A.: Time- and reduction-dependent rise of photosystem II fluorescence during microseconds-long inductions in leaves. – Photosynth. Res. **145**: 209-225, 2020.

Papageorgiou G.C., Govindjee (ed.): Chlorophyll *a* Fluorescence: A Signature of Photosynthesis. Pp. 818. Springer, Dordrecht 2004.

Papageorgiou G.C., Govindjee: Photosystem II fluorescence: Slow changes – Scaling from the past. – J. Photoch. Photobio. B **104**: 258-270, 2011.

Prášil O., Kolber Z.S., Falkowski P.G.: Control of the maximal chlorophyll fluorescence yield by the Q_B binding site. – Photosynthetica **56**: 150-162, 2018.

Reifarth F., Christen G., Seeliger A.G. *et al.*: Modification of the water oxidizing complex in leaves of the *dgd1* mutant of *Arabidopsis thaliana* deficient in the galactolipid digalactosyldiacylglycerol. – Biochemistry-US **36**: 11769-11776, 1997.

Rutherford A.W.: Photosystem II, the water-splitting enzyme. – Trends Biochem. Sci. **14**: 227-232, 1989.

Sakurai I., Mizusawa N., Wada H. *et al.*: Digalactosyldiacylglycerol is required for stabilization of the oxygen-evolving complex in photosystem II. – Plant Physiol. **145**: 1361-1370, 2007.

Sakurai I., Shen J.R., Leng J. *et al.*: Lipids in oxygen-evolving photosystem II complexes of cyanobacteria and higher plants. – J. Biochem. **140**: 201-209, 2006.

Schansker G., Tóth S.Z., Holzwarth A.R., Garab G.: Chlorophyll *a* fluorescence: Beyond the limits of the Q_A model. – Photosynth. Res. **120**: 43-58, 2014.

Schansker G., Tóth S.Z., Kovács L. *et al.*: Evidence for a fluorescence yield change driven by a light-induced conformational change within photosystem II during the fast chlorophyll *a* fluorescence rise. – BBA-Bioenergetics **1807**: 1032-1043, 2011.

Schreiber U., Bilger W., Neubauer C.: Chlorophyll fluorescence as a nonintrusive indicator for rapid assessment of in vivo photosynthesis. – In: Schulze E.-D., Caldwell M.M. (ed.): Ecophysiology of Photosynthesis. Pp. 49-70. Springer, Berlin-Heidelberg 1995.

Sebban P., Wraight C.A.: Heterogeneity of the $P^+Q^-_A$ recombination kinetics in reaction centers from *Rhodopseudomonas viridis*: the effects of pH and temperature. – BBA-Bioenergetics **974**: 54-65, 1989.

Shen J.R., Inoue Y.: Binding and functional properties of two new extrinsic components, cytochrome *c*-550 and a 12-kDa protein, in cyanobacterial photosystem II. – Biochemistry-US **32**: 1825-1832, 1993.

Shen J.R., Kamiya N.: Crystallization and the crystal properties of the oxygen-evolving photosystem II from *Synechococcus vulcanus*. – Biochemistry-US **39**: 14739-14744, 2000.

Shen J.R., Kawakami K., Koike H.: Purification and crystallization of oxygen-evolving photosystem II core complex from thermophilic cyanobacteria. – In: Carpentier R. (ed.): Photosynthesis Research Protocols. Methods in Molecular Biology (Methods and Protocols). Vol. 684. Pp. 41-51. Humana Press, Totowa 2011.

Shibata Y., Nishi S., Kawakami K. *et al.*: Photosystem II does not possess a simple excitation energy funnel: time-resolved fluorescence spectroscopy meets theory. – J. Am. Chem. Soc. **135**: 6903-6914, 2013.

Shlyk-Kerner O., Samish I., Kaftan D. *et al.*: Protein flexibility acclimatizes photosynthetic energy conversion to the ambient temperature. – Nature **442**: 827-830, 2006.

Siefermann D., Yamamoto H.Y.: Light-induced de-epoxidation of violaxanthin in lettuce chloroplasts IV. The effects of electron-transport conditions on violaxanthin availability. – BBA-Bioenergetics **387**: 149-158, 1975.

Sipka G., Magyar M., Mezzetti A. *et al.*: Light-adapted charge-separated state of photosystem II: Structural and functional dynamics of the closed reaction center. – Plant Cell **33**: 1286-1302, 2021.

Sipka G., Müller P., Brettel K. *et al.*: Redox transients of P680 associated with the incremental chlorophyll-*a* fluorescence yield rises elicited by a series of saturating flashes in diuron-treated photosystem II core complex of *Thermosynechococcus vulcanus*. – Physiol. Plantarum **166**: 22-32, 2019.

Sirohiwal A., Neese F., Pantazis D.A.: Chlorophyll excitation energies and structural stability of the CP47 antenna of photosystem II: a case study in the first-principles simulation of light-harvesting complexes. – Chem. Sci. **12**: 4463-4476, 2021.

Stirbet A.: Excitonic connectivity between photosystem II units: what is it, and how to measure it? – Photosynth. Res. **116**: 189-214, 2013.

Strasser R.J., Srivastava A., Govindjee: Polyphasic chlorophyll-*a* fluorescence transient in plants and cyanobacteria. – Photochem. Photobiol. **61**: 32-42, 1995.

Szczepaniak M., Sander J., Nowaczyk M. *et al.*: Charge separation, stabilization, and protein relaxation in photosystem II core particles with closed reaction center. – Biophys. J. **96**: 621-631, 2009.

Tang D.M., Jankowiak R., Seibert M., Small G.J.: Effects of detergent on the excited-state structure and relaxation dynamics of the photosystem II reaction center: A high-resolution hole burning study. – Photosynth. Res. **27**: 19-29, 1991.

Tiede D.M., Vázquez J., Córdova J., Marone P.A.: Time-resolved electrochromism associated with the formation of quinone anions in the *Rhodobacter sphaeroides* R26 reaction center. – Biochemistry-US **35**: 10763-10775, 1996.

Tóth S.Z., Schansker G., Strasser R.J.: A non-invasive assay of the plastoquinone pool redox state based on the OJIP-transient. – Photosynth Res **93**: 193-203, 2007.

Umena Y., Kawakami K., Shen J.R. *et al.*: Crystal structure of oxygen-evolving photosystem II at a resolution of 1.9 Å. – Nature **473**: 55-60, 2011.

Valkunas L., Geacintov N.E., France L., Breton J.: The dependence of the shapes of fluorescence induction curves in chloroplasts on the duration of illumination pulses. – Biophys. J. **59**: 397-408, 1991.

van der Weij-de Wit C.D., Dekker J.P., van Grondelle R., van Stokkum I.H.M.: Charge separation is virtually irreversible in photosystem II core complexes with oxidized primary quinone acceptor. – J. Phys. Chem. A **115**: 3947-3956, 2011.

Vredenberg W.J.: Analysis of initial chlorophyll fluorescence induction kinetics in chloroplasts in terms of rate constants of donor side quenching release and electron trapping in photosystem II. – Photosynth. Res. **96**: 83-97, 2008.

Vredenberg W.: A simple routine for quantitative analysis of light and dark kinetics of photochemical and non-photochemical quenching of chlorophyll fluorescence in intact leaves. – Photosynth. Res. **124**: 87-106, 2015.

Vredenberg W., Prasil O.: On the polyphasic quenching kinetics of chlorophyll *a* fluorescence in algae after light pulses of variable length. – Photosynth. Res. **117**: 321-337, 2013.

Yamamoto H.Y., Higashi R.M.: Violaxanthin de-epoxidase: Lipid composition and substrate specificity. – Arch. Biochem. Biophys. **190**: 514-522, 1978.